Geophysica (1987), Vol. 23, No. 1, pp. 35–46
Printed in Finland

550.9410S

EISCAT AS A RADAR FOR AURORAL RESEARCH – A CASE STUDY

by

A. HUUSKONEN and J. KANGAS

Department of Physics, University of Oulu
SF–90570 Oulu, Finland

T. TURUNEN

EISCAT Scientific Association
S–98127 Kiruna, Sweden

Abstract

EISCAT incoherent scatter radar system has been designed primarily to study the auroral ionosphere. Using the most modern modulation technique high-resolution measurements of physical parameters of auroral arcs can be made. In particular due to the tristatic nature of the radar the electric field pattern within the arc can be derived. As an example of EISCAT auroral experiments we show results from a special Finnish experiment called EFOR-V4 which was run on Nov 17–18, 1983. We observe most of the time a particle E-layer below 100 km altitude which often disappears before an arc. Electric fields at 172 km altitude and electron density profiles are investigated, especially in the case of a westward moving arc occurring soon after 21 UT. At the leading edge of the arc the electron density profile is characterized by a double structure: electron density peaks at 88 and 115 km. This structure disappears inside the arc. We conclude that the energy spectrum of precipitating electrons changes dramatically within the arc. Electric field measurements related to the same arc show that the electric field has a westward component in front of the arc. Inside the arc the field turns eastwards. It is found that both the polarization electric fields and the field-aligned currents maintain the current continuity across the arc.

1. *Introduction*

Auroral arc is the basic form of visual auroras. The most simple form is a homogeneous east-west oriented quiet arc which is intensified and distorted during auroral substorms. In order to understand the acceleration of incident auroral particles, electric fields and characteristics of precipitating particles are to be measured. Several techniques as ionized clouds, rockets, radars and satellites have been used for such measurements.

De la BEAUJADIÈRE *et al.* (1977, 1981) have systematized the Chatanika radar observations of auroral arcs according to the patterns of the meridional electric field across the arc. They identify four types of arcs:

(1) The anticorrelation type where the northward field decreases within the arc.
(2) The correlation type where the southward electric field intensifies within the arc.
(3) The asymmetric type where the northward electric field is large on the equatorward side of the arc, decreases within the arc and remains small on the poleward side of the arc.
(4) The reversal type where the electric field changes its sign within the arc.

This classification of arcs is mainly based on morphological features. MARKLUND (1984) has proposed a more physical classification scheme which takes into account the relative influence of polarization electric fields and field-aligned currents on the electric field pattern. Both of these can maintain the current continuity across the arc. In this method, the observed electric field pattern within the arc is compared with that estimated from the current continuity equation assuming no field-aligned currents. The tangential electric field is to be known in these calculations. By using the method, Marklund has been able to group the arcs into three main categories: Polarization arcs, Birkeland current arcs and Combination arcs.

In this paper, we discuss the use of the EISCAT incoherent radar to investigate the physics of auroral arcs. The EISCAT UHF-radar is tristatic and some shortcomings of monostatic radars can be avoided. A recent description of the EISCAT system is given by FOLKESTAD *et al.* (1983). As a concrete example we show results from a Finnish EISCAT experiment called EFOR-V4 which was run on November 17–18, 1983 from 19 UT to 6 UT. During the night several auroral arcs were observed in the radar beam. An especially interesting case is a westward moving auroral arc which appears in the radar beam after 21.07 UT. The arc is oriented in a north-south direction and is associated with a substorm activity. The internal structure of the arc as well as the electric field pattern and the currents inside and near the arc are discussed.

2. *Auroral arc measurements by the EISCAT radar*

In auroral arc measurements by the EISCAT UHF-radar a fixed antenna geometry is often used. In this geometry the transmitter antenna at Tromsø points to a direction near the local magnetic field line and the remote antennas at Sodankylä and Kiruna stare to a point in the F-layer. During the measurement, the experimentor waits for auroral arcs, which often are moving with a considerable speed, to drift through the radar beam. When this happens, one can by using the Tromsø data measure the electron density profile in different parts of the arc. Also by combining data from all stations the electric field both inside and near the arc can be measured. A typical time resolution is of the order of a few tens of seconds but, in favourable conditions, plasma parameters can be measured well in five seconds. The direction of the arc motion which is important for the interpretation of measurements cannot directly be obtained from the EISCAT-data. For this purpose one can use All Sky Camera (ASC) pictures.

A fixed geometry, however, is not suitable for all auroral studies. It may happen that the arcs are stationary or the active auroras stay well to the north or to the south of Tromsø. In these cases the fixed antenna configuration may not see the auroras at all whereas a measurement where the transmitter antenna is pointed to many directions in the meridional plane (a latitude scan) would more probably find the auroras. A latitude scan has, on the other hand, its drawbacks. During antenna movement, which takes about 20 seconds, reliable measurements are not possible. Also the measurements in successive points, usually 25–50 km apart, cannot easily be related in the case of active auroras. A latitude scan is well suited for studies of wide-spread diffuse auroras but active auroras are more efficiently studied if one fixes the antenna and lets the auroras move.

3. *The experiment EFOR-V4*

In the present experiment the radar beam was held fixed towards south at an elevation angle of 89 degrees. The remote antennas of Kiruna and Sodankylä were oriented to a common volume at 172 km. Thus the geometry of the experiment was not exactly field-aligned. This can lead to some difficulties which are discussed later.

The pulse modulation pattern of the monostatic part of the transmission is shown in Fig. 1. It consists of four four-pulse codes and two short pulses. The pulse length of 20 μs results in a peak-to-peak resolution of 6 km but most of the signal contribution comes from a volume of 3 km in length along the beam. For the remote sites, a long pulse of 330 μs was transmitted. The basic inter-

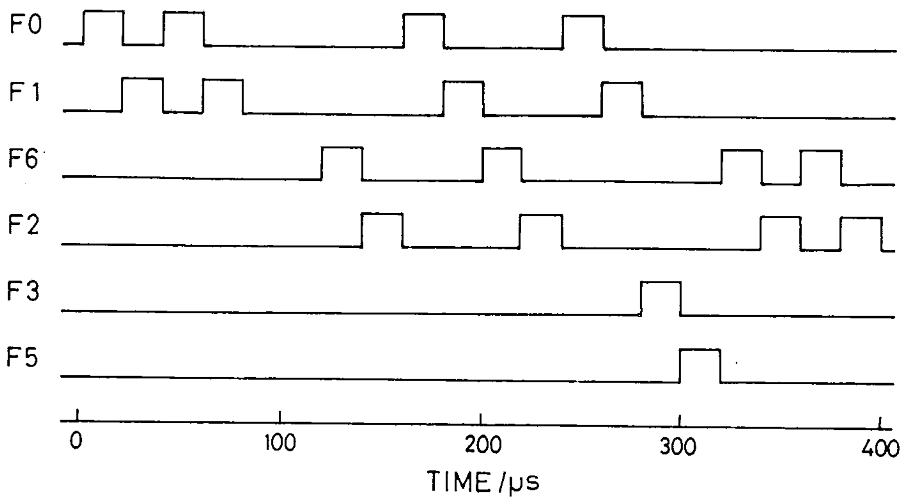

Fig. 1. Pulse modulation pattern of the monostatic part of the EFOR-V4 experiment.

gration time is 10 seconds. With this modulation the plasma autocorrelation function is measured in a number of range gates. The various plasma parameters, electron density, electron temperature, ion temperature, ion-neutral collision frequency, ion velocity and ion composition are calculated from the measured autocorrelation functions by a non-linear least square fit method.

Electron density profiles are obtained using the deconvolution method introduced by LEHTINEN and HUUSKONEN (1986). In this method the multipulse zero lag information is combined with that of separate single pulses. The channel balancing is done by using the background and calibration measurements. The combined pulse code and single pulse powers are corrected for range and converted to electron densities by applying a radar constant and an assumed electron to ion temperature ratio equal to one. This procedure is thought to be good enough for purposes of this paper.

Doppler shifts are estimated by the matched filter velocity fit method. Because the pulse codes failed to give reliable estimates of Doppler shifts at the altitude of the common volume and the long pulse was not received at Tromsø, the two shifts of the remote sites are combined to give a velocity vector assuming a null ion velocity along the magnetic field. Finally, the velocity vector is rotated 90 degrees to get the perpendicular electric field.

4. *Observations*

The experiment was run during very active auroral conditions. A strong magnetic activity started at about 18 UT and was most intense between 20 and 22 UT. Fig. 2 shows magnetograms from the north-south chain of the EISCAT-magnetometers in northern Finland and Norway. The most interesting event of the present study occurs at about 21 UT when the *Y* component turns positive indicating a southward directed current in the ionosphere.

An all-sky camera was operated at Kilpisjärvi (KIL) at a rate of 3 frames per minute. Unfortunately most of the night was cloudy and only a few photos are available for interpretation. A rectified all-sky camera image taken at 21.05.43 UT is shown in Fig. 3 on a map which shows also the locations of EISCAT-sites and EISCAT-magnetometer stations. Two mainly north-south oriented auroral arcs are identified. By 21.07.03 UT the arcs move westwards and disappear behind the clouds. This westward movement of the precipitation area is further confirmed by riometer recordings from Kevo (KEV) and Kilpisjärvi. A sharp increase of absorption starts at Kevo at 21.02 UT and at Kilpisjärvi at 21.05.30 UT. This corresponds to a westward velocity of about 1.2 kms^{-1}. The increase was preceded by a deep minimum of absorption during 2 to 3 minutes, especially at Kilpisjärvi.

Fig. 4 shows the contours of constant electron density from 20.40 to 22.10 UT. Two kinds of structures are recognized. First, a particle E-layer is seen nearly continuously below the altitude of 100 km. This indicates the presence of diffuse

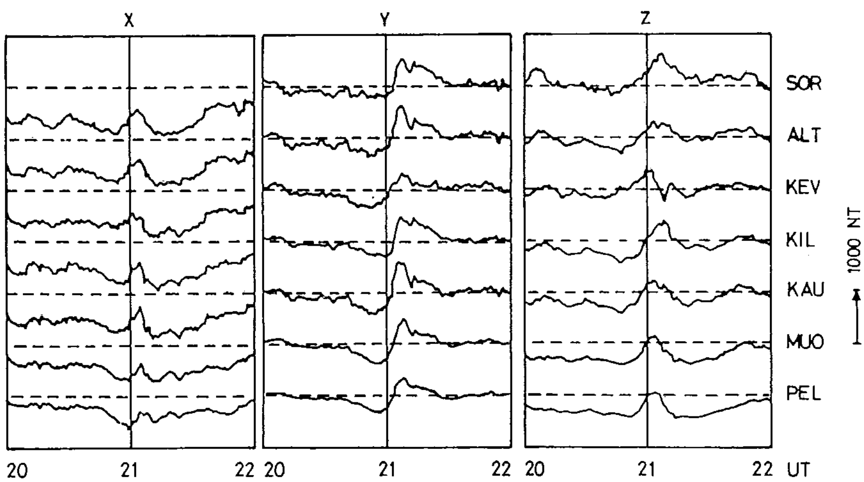

Fig. 2. Magnetic variations recorded at seven EISCAT magnetometer stations on November 17, 1983 from 20 to 22 UT. Abbreviations and locations of the stations are shown in Fig. 3.

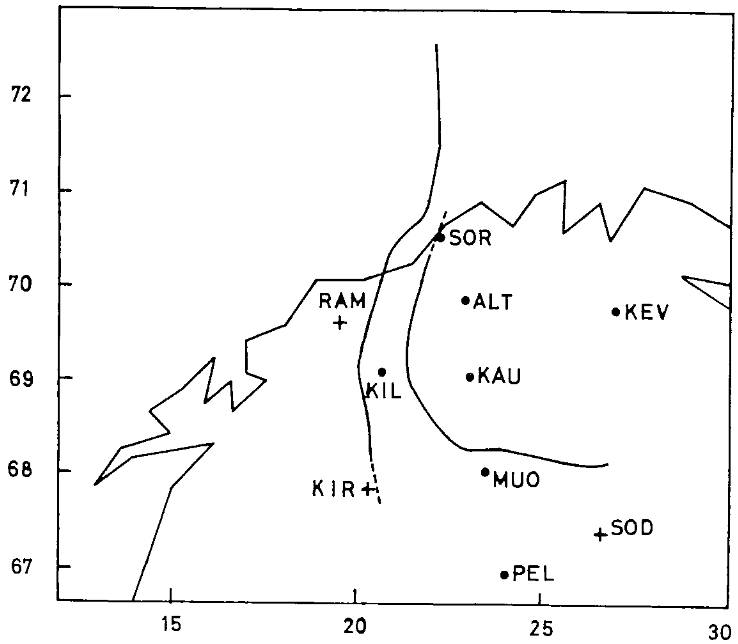

Fig. 3. Rectified all-sky camera image at 21.05.43 UT where two north-south oriented auroral arcs are seen. Abbreviations: SOR = Sørøya, ALT = Alta, KAU = Kautokeino, MUO = Muonio, PEL = Pello, KEV = Kevo, KIL = Kilpisjärvi, RAM = Ramfjordmoen, KIR = Kiruna and SOD = Sodankylä.

auroras with a large horizontal extent but which cannot be identified in all-sky camera pictures because of clouds. Secondly, the vertical structures of enhanced electron density are related to auroral arcs which hit the radar beam. This is confirmed by the observations after 21.07 UT when the arcs shown in Fig. 3 drift through the beam. It is noticed that an arc is often preceded by a weakening of the background particle layer. The most prominent gap appears before the arc at 21.07 UT.

Some characteristics of the two auroral layers are illustrated in Fig. 5 which shows a few electron density profiles at the western edge of the arc at about 21.07 UT. The first clear signature of the arc is seen in the lower E region at about 85 km at 21.07.01 UT. By 21.07.21 UT this layer has intensified and moved to about 88 km but at the same time another enhancement occurs at 115 km. This double structure of the E region disappears by 21.07.41 UT. The lower F-region is weak in the first three profiles in Fig. 5 but intensifies by 21.07.41 UT. This indicates that the arc has not been exactly in the meridional plane.

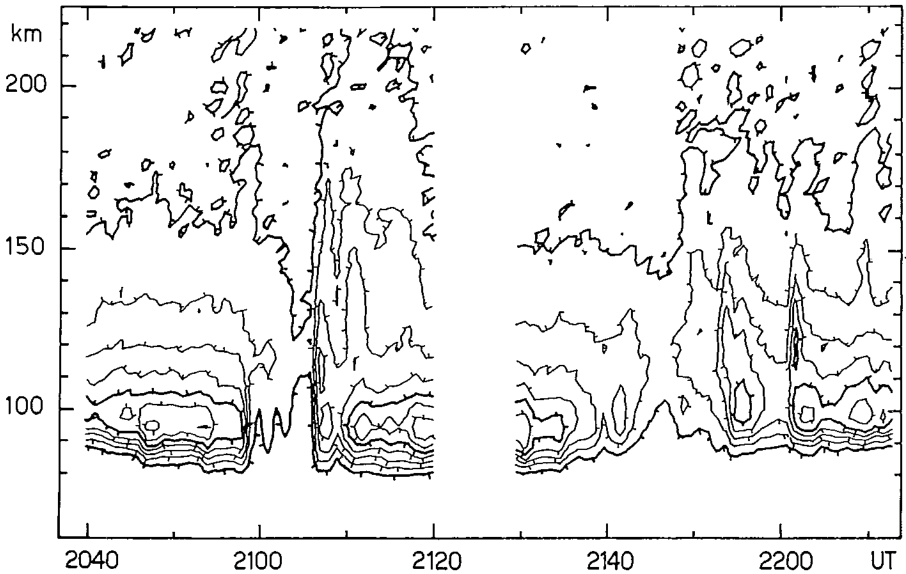

Fig. 4. Contours of constant electron density from 20.40 to 22.10 UT on Nov 17, 1983. The outermost line corresponds to an electron density of $5 \cdot 10^{10}$ m^{-3} and the step is $5 \cdot 10^{10}$ m^{-3}. The integration time is 30 seconds. Data between 21.20 and 21.30 UT was lost during a change of tape.

The results of the electric field analysis from 20.57 UT to 21.12 UT are presented in Fig. 6 together with the height integrated Hall conductivity. The zonal component of the electric field shows a smoother behaviour than the meridional one. This difference in smoothness is probably due to the better signal-to-noise ratio (SNR) at Kiruna than at Sodankylä and the fact that the zonal component is determined mainly by the Doppler shift measured at Kiruna whereas the two remote sites have nearly equal weights in the meridional component.

The zonal component decreases inside the arcs which occur at 20.59, 21.01 and 21.04 UT. The presence of auroral arcs cannot be proved by optical observations due to the clouds but the Hall conductivity enhances clearly at these times. The decrease of the zonal component cloud mean that the arcs are oriented in the east-west direction but other explanations are also possible. As the north-south oriented arc approaches the radar beam after 21.07 UT the zonal component points westwards but turns eastwards later when the arc is already within the beam. After the passage of the arc the field turns back westwards at 21.09 UT. The field change as well as the conductivity gradient is smaller at the eastern edge of the arc at the western edge.

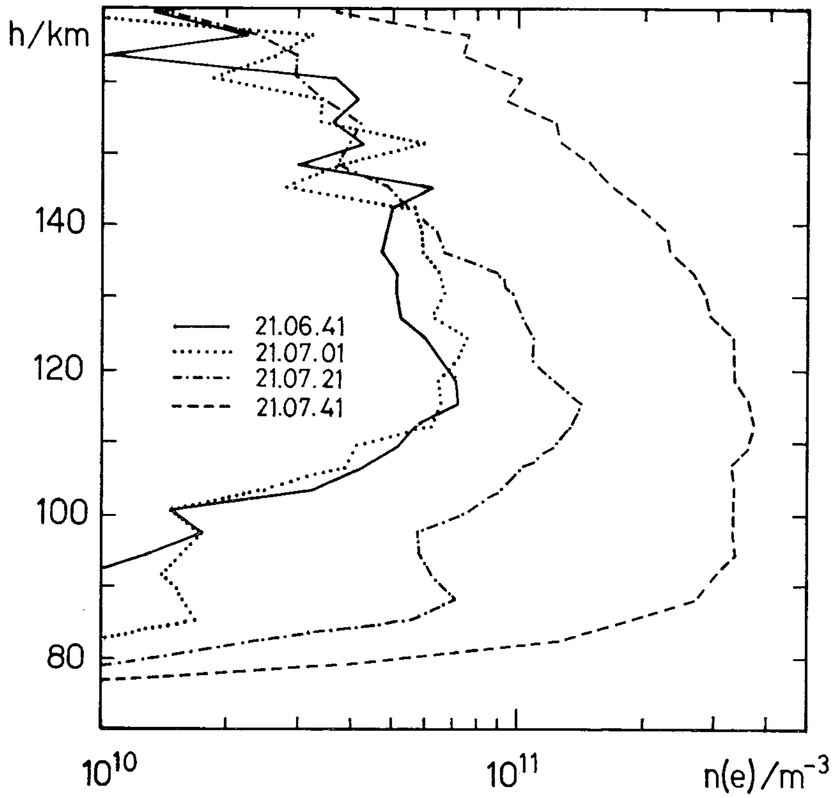

Fig. 5. Electron density profiles displaying the entering of the auroral arc into the radar beam at 21.07 UT. The times displayed in the figure give the end of the integration period of 10 seconds.

5. *Discussion*

The results of this study show that the EISCAT experiment described here is useful for measuring some of the physical parameters of auroral arcs with a high resolution. Electron density profiles can be obtained with resolutions of 10 seconds and 3 km in time and height, respectively. The deconvolution of the zero lags of the pulse codes as described by LEHTINEN and HUUSKONEN (1986) has been an essential improvement of the data analysis in this respect. A typical width of an auroral E-layer is 10–50 km (see Fig. 5 or *e.g.* REES, 1963 or HUUSKONEN *et al.*, 1984) and only at the bottom of the layer the electron density can change remarkably within one gate. So the altitude resolution that is obtained with this code is suitable for measuring the electron density profile of particle E-layer. If one wants

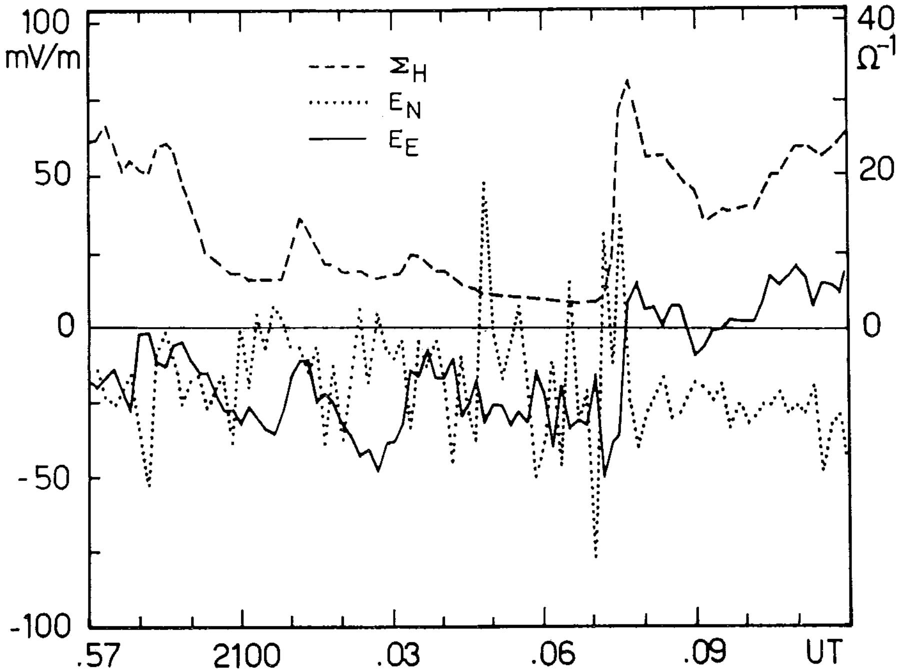

Fig. 6. Variations of the north and east component of the electric field measured by EISCAT at the altitude of 172 km from 20.57 UT to 21.12 UT on Nov 17, 1983. Increases in the height integrated Hall conductivity indicate the presence of electron precipitation event within the radar beam. The integration time is 10 seconds.

to measure with a better height resolution, the use of phase codes can give a resolution as good as 300 meters.

The ion velocity vector, needed for the determination of the electric field, is obtained at the common volume by measuring one component of the vector at each of the three sites. In this experiment the common volume was situated at 172 km whereas *e.g.* in the EISCAT Common Program (CP) experiments it lies above 300 km. When the experiment was run on Nov 17, 1983 all eight transmitter channels were available but only six of the eight receiver channels could be used at Tromsø. All these were reserved to the pulse codes and short pulses to get best possible determination of the plasma parameters in the E-layer and so the long pulse was utilized only at the remote sites. This placed a severe restriction on the altitude of the common volume because the pulse codes can hardly give any detectable signals above 200 km. Thus the common volume should be placed at the lowest possible altitude.

On the other hand, the effect of ion-neutral collisions on the ion motion increases with decreasing altitude and the electric field is not easily derivable from the ion velocity below a certain altitude, say 160 km. The altitude of 172 km was chosen as a good compromise because one can expect to get reliable estimates of the ion velocity during periods of high electron density and the collisions do not have much influence on the ion motion. Actually no reliable estimates of the ion velocity were obtained from the pulse code data and the ion velocity has to be estimated from the remote data only as described in section 3. Nowadays the situation is quite different and one can combine in one and the same experiment both a good determination of the plasma parameters in the E-layer and a good determination of the electric field in the F-layer. In new versions of the present experiment called GEN-8 and GEN-9 the common volume is situated at an altitude of 250 km (see TURUNEN, 1985).

To investigate the relative importance of the field-aligned currents and the polarization electric fields, the eastward component of the height-integrated current density is calculated in front of the arc, inside the arc and behind the arc. These three regions correspond to time periods of 21.06–21.07, 21.08–21.09 and 21.09–21.10, respectively. If the northward current can be assumed to be constant along the arc, differences of the eastward currents are equal to field-aligned currents. The constancy of the northward currents in this case is supported by the similarity of the Y-component at all EISCAT magnetometer cross stations (Fig. 2). Using the values 3.6, 20.8 and 15.4 Ω^{-1} for the height-integrated Hall conductivity, 1.9, 6.0 and 4.4 Ω^{-1} for the height-integrated Pedersen conductivity, −28.2, 2.1 and 0.4 mV/m for the E-component of the electric field and −28.0, −22.5 and −25.0 mV/m for the N-component of the electric field, height-integrated eastward current densities of −150, −450 and −380 mA/m are obtained in the three regions, respectively. The result shows that intense upward field-aligned currents flow at the leading edge of the westward moving arc.

The double reversal of the electric field across the arc is caused by a polarization electric field. This polarization field together with the field-aligned currents maintain the current continuity across the arc. If we compare these results with the classification scheme proposed by MARKLUND (1984) it seems impossible to place the present arc to any well-defined subcategory typified by Marklund. It has to be noticed that Marklund studied mostly east-west oriented quiet arcs whereas we are studing a moving north-south oriented arc.

The electronic field was found to point away from the leading edge of the westward propagating arc which suggests that these westward moving arcs differ from the westward travelling surge (WTS) which is the optical signature of the substorm expansion. It has been shown that the electric field associated with a

WTS points towards the center of the surge (OPGENOORTH, 1983). However, it may be significant that we obtain here a value of 1.2 kms^{-1} for the westward velocity of the precipitation region which is also a typical velocity of the WTS.

At first sight Fig. 6 would indicate that the conductivity is enhanced before the field turns and that the westward field penetrates into the arc at 21.07 UT. This effect is caused by the non-field-aligned geometry of the present experiment which may create a time lagt between the conductivity measurement done at the E-layer and the electric field measurement at the lower F-layer. Fig. 5 shows that this is indeed the case. In this respect the SNR measured at the common volume would be a better way of displaying the precipitation regions. Inside the gap, however, the SNR is low and the integrated conductivity is a better indicator of arcs. A look at the SNR measured at the common volume shows that the field turns just at the arrival of the arc.

It is obvious that the energy spectrum of precipitating electrons at the western edge of the precipitation region has a double structure. The lower enhancement below 90 km corresponds to the ionization produced by primary electrons with a characteristic energy of 50–60 keV whereas the maximum at about 115 km can be related to the electron energies of 5 to 7 keV (see REES, 1964). The situation lasts for about 30 seconds after which an intense precipitation occurs throughout the whole E-region and the double structure cannot be identified any more. Thus the spectrum of precipitating electrons may change drastically within an arc.

The enhanced layer below the 100 km altitude produced by high-energy electrons remains quite stable during most of the active period analyzed here. However, it sometimes weakens or even disappears before the appearance of the auroral arc produced by lower energy electrons. The gaps are probably caused by a weaker precipitation near the arcs. When the precipitation stops the ionosphere gets gradually empty because of recombination. Also the large electric fields near auroral arcs can remove the ionization. The question about the reason for the weaker precipitation near auroral arcs remains still open.

Acknowledgements: The EISCAT Scientific Association is supported by the Centre National de la Rescherche Scientifique of France, Suomen Akatemia of Finland, Max-Planck Gesellschaft of West Germany, Norges Almenvitenskaplige Forskningsråd of Norway, Naturvetenskapliga Forskningsrådet of Sweden and Engineering Research Council of the United Kingdom. The authors are grateful to the Finnish Meteorological Institute for the all-sky camera pictures and the EISCAT-magnetometer cross data.

REFERENCES

DE LA BEAUJARDIÈRE, O., VONDRAK, R., and M. BARON, 1977: Radar observations of electric fields and currents associated with auroral arcs. *J. Geophys. Res.*, 82, 5051–5062.

–»– , VONDRAK, R., HEELIS, R., HANSON, W., and R. HOFFMAN, 1981: Auroral arc electrodynamic parameters measured by AE-C and the Chatanika radar. *J. Geophys. Res.*, 86, 4671–4685.

FOLKESTAD, K., HAGFORS, T., and S. WESTERLUND, 1983: EISCAT: An updated description of technical characteristics and operational capabilities. *Radio Sci.*, 18, 867–879.

HUUSKONEN, A., NYGRÉN, T., JALONEN, L., and J. OKSMAN, 1984: The effect of electric field-induced vertical convection on the precipitation E-layer. *J. Atmos. Terr. Phys.*, 46, 927–935.

LEHTINEN, M., and A. HUUSKONEN, 1986: The use of multipulse zero lag data to improve incoherent scatter radar power profile accuracy. J. Atmos. Terr. Phys., 48, 787–793.

MARKLUND, G., 1984: Auroral arc classification scheme based on the observed arc-associated electric field pattern. *Planet. Space Sci.*, 32, 193–211.

OPGENOORTH, H.J., PELLINEN, R.J., BAUMJOHANN, W., NIELSEN, E., MARKLUND, G., and L. ELIASSON, 1983: Three-dimensional current flow and particle precipitation in a westward travelling surge (observed during the BARIUM-GEOS rocket experiment). *J. Geophys. Res.*, 88, 3138–3152.

REES, M.H., 1963: Auroral ionization and excitation by indicent energetic electrons. *Planet. Space Sci.*, 11, 1209–1218.

–»– , 1964: Note on the penetration of energetic electrons into the earth's atmosphere. *Ibid.*, 12, 722–725.

TURUNEN, T., 1985: The GEN-system for the EISCAT incoherent scatter radars. *EISCAT Technical Note* 85/44.